*Pak. J. Engg. Appl. Sci. Vol. 26 January, 2020 (p. 1–15)*

# The use of GIS and Geo-electric Techniques for Delineation Surface and Groundwater Potential in Kotli City, District Kotli, Azad Jammu and Kashmir, Pakistan

Abrar Niaz*, Mubashar Imtiaz, Muhammad Rustam Khan, Fahad Hameed, Jawad Niaz, Ali Yousaf Khan, Kishwar Mehmood

*Institute of Geology, University of Azad Jammu and Kashmir, Muzaffarabad, P.O Box 13100, Azad Jammu and Kashmir, Pakistan*

* **Correspondence Author:** Email: abrar.niaz@ajku.edu.pk

## Abstract

*The geo-electrical and Geographic Information System (GIS) techniques have been employed for modeling surface and groundwater bodies of the Kotli city and its surrounding areas in the District Kotli, Azad Jammu and Kashmir, Pakistan. The Landsat 8 imagery is used for modeling the surface water and Vertical Electrical Sounding (VES) method is applied for the delineation of subsurface lithology in the study area. A total number of 21 VES points have been collected by using Schlumberger configuration. The VES data was collected using ABEM Terrameter SAS 4000. The acquired data have been processed by using IPI2WIN (2008) software and the interpretation was carried out in terms of true resistivity and thickness of different layers of sedimentary strata. The groundwater potential zones (good and moderate) have been identified in the area. The thickness of aquifer varies from 20 m to 129 m. Most of aquifers are confined and of "A" ($\rho_1 < \rho_2 < \rho_3$), "K" ($\rho_1 < \rho_2 > \rho_3$) and "H" type ($\rho_1 > \rho_2 < \rho_3$). The VES 1, 2, 10, 11, 12, 20 and 21 south western part of the study area showed poor to weak overburden protective capacity of the aquifers, hence are vulnerable to infiltrating fluids from storage facility or dumps.*

**Key Words:** Vertical Electrical Sounding, Geographic Information System, Environment for Visualizing Image, Digital Elevation Model

## 1. Introduction

The water scarcity is the major problem in most of the areas of Pakistan. With growing population, the demands of water supply has increased many folds. The study was conducted in the Kotli city area of District Kotli Azad Jammu & Kashmir, Pakistan. The area is moderately populated and most of its population depends upon the groundwater for irrigation and domestic use. The peoples are involved in blind drilling of water wells and investing huge money and time. Most of well failed due to lack of scientific study [1], [2]. The integrated electrical resistivity method and Geographic Information System (GIS) have been used for delineation of aquifers and selection of appropriate sites for installation of tube wells. In addition, it is cost effective approach for the evaluation of subsurface geological structure of the area [3], [4]. The GIS tool provides the suitable management of complex data [5]. Rapid analysis of the spatial data and different layers integration is possible in GIS software. The GIS tool is used to develop numerical modeling of groundwater, presentation and integration of the image processing and modeling results [6].

The VES technique was chosen in the selected area using Schlumberger configuration as the geoelectrical technique is used for delineation of thickness, boundary and depth of an aquifer [7], [8], in delineation of aquifer potential by using Rockworks software [9], investigation of geothermal reservoirs [10] and hydraulic conductivity assessment of aquifer. Vertical alterations of the resistivity of the subsurface layers are measured by VES. This technique has been proven to a greater extent for hydrogeological investigation of sedimentary basin [11], [12].

Geophysics, particularly vertical electrical soundings techniques have been commonly used for a wide range of geotechnical and groundwater problems [13], [14], [15], [16]. Besides, it can likewise be utilized either as a part of the type of vertical electrical soundings (VES's) or even profiling to look for groundwater in both permeable and fissured media channels [17],[18], [19].

At present, community of Sehnsa and adjoining areas use the bore water although Government has also inaugurated various projects to consummate the need of the community [20]. These projects do not achieve the increasing requirement of growing population. Consequently, this research work contributed to know the hydrological characteristics of the area, documentation of aquifer type, the analysis of depositional model of the study area, locating and reporting of fresh water supply.

## 1.1 Location of Study Area

The study area comprises of Kotli city and its adjoining areas which are situated in District Kotli, Azad Jammu and Kashmir, Pakistan. The area lies between latitude 33°30'7.80" N to 33°29'38.16" N and longitude 73°52'54.60" E to 73°55'48.66" E in the Kotli city (Fig.1). The integrated study techniques have been used for identification of surface and groundwater resources in the area.

## 1.2 Geological setting of the study area

Geologically, the study area is located in Kashmir Basin. The area under investigation basically lies in the Sub-Himalayas tectonically and generally comprises of mainly molasse deposits named as Siwaliks. The study area comprises of the Rawalpindi Group of rocks. The stratigraphic formations which are exposed in the study area Middle to Early Miocene Kamlial Formation, Early Miocene Murree Formation and Recent Quaternary Alluvium (Fig. 1) [21].

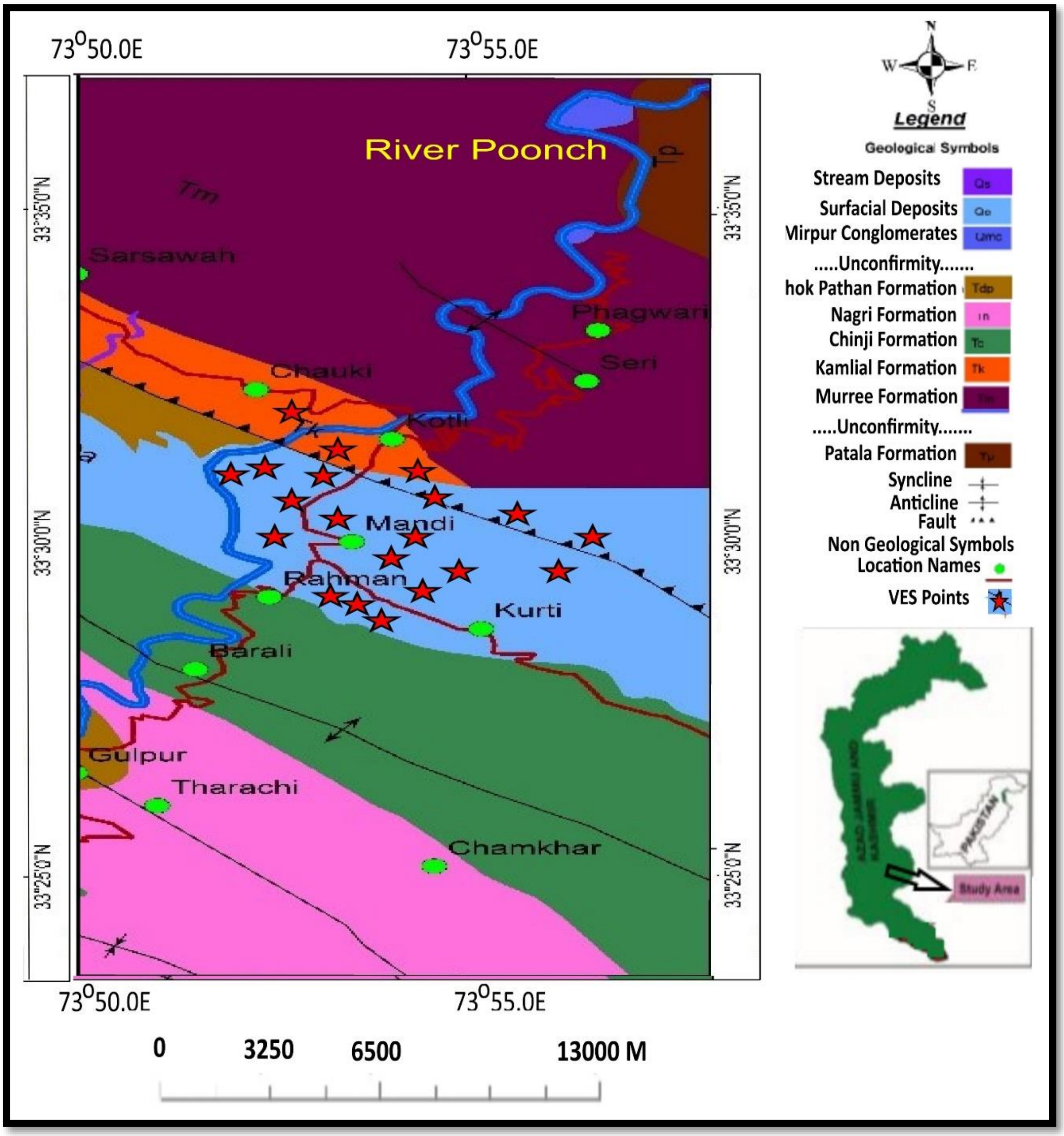


**Fig. 1:** Regional geological and location map of the area, compiled after GSP, 2000

The Murree Formation is composed of monotonous sequence of purple clay, dark red and purple grey, greenish grey sandstone with subordinate intraformational conglomerate. The Murree Formation also consist of cyclic deposition of sandstone and Clay. This sequence is very important for groundwater development in the area and form confine type aquifer. The formation is well exposed on north-eastern part of the study area. The Kamlial Formation is composed dominantly of sandstone, siltstone, shale and mudstone. The sandstone is hard and compact. The formation is widely exposed in the north-western part of the study area [21]. The surficial deposits are mainly river deposits comprises of gravels, boulders, intercalation of sand and clay. The wind-brown sand, alluvial fans, recent flood plain deposits, lacustrine deposits are also present in the area.

## 1.3 Hydrogeology of the area

The study area under observation dominantly comprises of clastic sedimentary rocks with clay, gravel and sand deposits. The water bearing strata consists of sand and gravel, boulder clay and sandy clay. The rainfall, nalas and seasonal tributaries are the major sources of recharge for aquifers in this area. The public health department drilled some wells in the area which are the limited source of water supply in the area. There is no significant previous studies related to hydrogeology of the area were found in this area. The river Poonch is also acting as the recharging agent for groundwater in the area. 1300 mm per year rainfall is recorded in the area.

## 2. Materials and Methods

The Terrameter SAS 4000 (Sweden) ABEM instrument with its accessories (including hammers, stainless electrodes, cables and measuring tape) was utilized for data acquisition in the area.

The 21 VES points were acquired by applying Schlumberger configuration with maximum electrode separation (AB/2) of 250 m (Fig. 1). In this configuration, the distance was symmetrically increased between electrodes for subsurface depth coverage.

The generated potential difference after applying current was measured with the help pair of electrode (potential electrode). The data was acquired in April 2017. The IPI2WIN (2008) iteration software was employed for processing the acquired data. The software automatically analyses the data from 1D geoelectric measurements at a single point with the smallest error to determine the true resistivity, depth and thickness of the subsurface geoelectric layers (IPI2WIN computer program 2000) [22], [23]. The Dar-Zarrouk parameters such as conductance, anisotropy, transverse resistance have been calculated. The land cover map was derived from Landsat 8 imagery by using Exelis ENVI (5.3) and Arc GIS (10.1) software. Qualitative interpretation have been done by using the field curve shape. The field curve was obtained by the plot of apparent resistivity with electrode spacing (Fig. 2) and master curves was employed for interpretation of the curves. The shapes of the curve revealed Q, A, H and K type curves. The subsurface layers distribution is as follows: Q type: $\rho1 > \rho2 > \rho3$, K type, $\rho1 < \rho2 > \rho3$; A type: $\rho1 < \rho2 < \rho3$ and H type, $\rho1 > \rho2 < \rho3$ demarcated the four layer curves, where $\rho$ indicate the true resistivity of the layer (Fig. 2). The iso-resistivity maps at different depths were made using Arc GIS (10.1) and Golden Software Surfer (11). with Arc GIS (10.1) and the Digital Elevation Model (DEM).

The 3D lithological fence diagrams and lithological models were made with the help of Rockworks (17) software. Finally, the topographic and drainage map of the study have been prepared.

## 3. Results

The IPI2WIN (2008) was used to iterate curves for each VES station. The smooth curves taken through the set of data points were interpreted quantitatively by the method of partial curve matching.

The analysis of data further reveals the typical three-layer VES curves. The thickness and resistivity of different layers were calculated at every VES point (Table 1) which indicates the presence of three to four geoelectrical layers in the subsurface. The geological layers consist of boulder clay, boulder and gravel, clay, dry sandy soil, gravel and sandstone of recent alluvium deposits (Table 1).

The higher resistivity range (15.65 to 29447 Ωm) at different locations in the second and third layers have been interpreted as a sandstone. There is evidence of groundwater potential in the second and third layers. Aquifer thickness map shows (Fig.11) that the aquifer thickness is high in the south-eastern parts of the study area that assures the adequate water potential. The known geological information on the surface lies closely to the bore hole data and computed geological model by Rockworks (17). The drainage pattern has been constructed using DEM image on GIS.

The area comprises of dendritic drainage pattern.

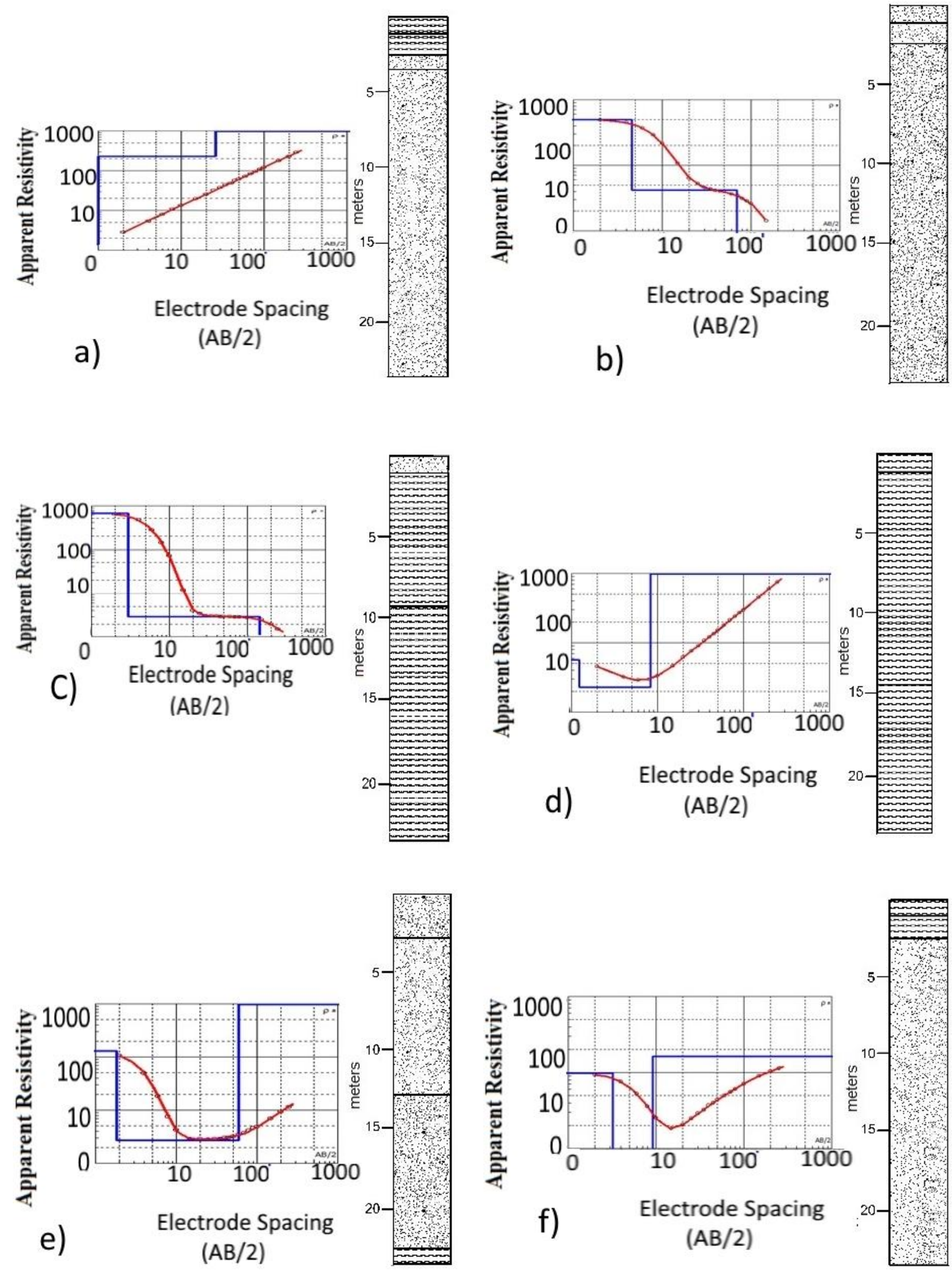


**Fig. 2:** The typical three-layered VES, 2,3,4,5,9,10 curves of the study area

**Table 1:** Interpretation of the data

| Latitude (N) | Longitude (E) | VES station | Curve Type | $\rho 1$ (Ωm) | h1 (m) | $\rho 2$ (Ωm) | h2 (m) | $\rho 3$ (Ωm) | h3 (m) | $\rho 4$ (Ωm) | Aquifer thickness (m) | Apparent resistivity at 30m (Ωm) | Apparent resistivity at 60m (Ωm) | Apparent resistivity at 90m (Ωm) | Longitudinal conductance (mhos) | Anisotropy (λ) |
|---|---|---|---|---|---|---|---|---|---|---|---|---|---|---|---|---|
| 73.52926 | 33.30225 | 1 | Q | 4269 | 1.41 | 117 | 2.67 | 0.985 | | | 2.67 | 2.3387 | 1.1971 | 1.5768 | 0.0231508 | 4.4028578 |
| 73.5291 | 33.3013 | 2 | KH | 0.302 | 1 | 4.59 | 2.79 | 0.563 | 10.6 | 8.16 | 10.6 | 4.4239 | 1.5204 | 2.9348 | 22.7468101 | 1.047741 |
| 73.54276 | 33.30897 | 3 | A | 3.62 | 1 | 8.99 | 2.79 | 442 | | | 2.79 | 66.823 | 167.42 | 1.3925 | 0.58658792 | 0.586055 |
| 73.53204 | 33.30733 | 4 | K | 34.7 | 1.21 | 35.8 | 0.815 | 10.3 | | | 0.815 | 25.374 | 12.954 | 9.4453 | 0.05763568 | 0.5001171 |
| 73.53822 | 33.30241 | 5 | K | 0.617 | 4.68 | 0.0971 | 8.2 | 38.8 | | | 8.2 | 2.7495 | 2.3847 | 5.6583 | 92.0341108 | 1.021835 |
| 73.5477 | 33.3178 | 6 | K | 91 | 0.824 | 91 | 1.24 | 24.7 | | | 1.24 | 84.737 | 30.141 | 23.965 | 0.02268132 | 0.5 |
| 73.54245 | 33.3146 | 7 | K | 5512 | 2.37 | 67023 | 8.15 | 90.5 | | | 8.15 | 261.04 | 511.805 | 2.7926 | 0.00055157 | 1.3937519 |
| 73.53577 | 33.31103 | 8 | A | 0.0036 | 1 | 0.111 | 2.62 | 0.959 | | | 2.62 | 439.15 | 3.0279 | 116.0963 | 301.381381 | 3.3856074 |
| 73.53907 | 33.30856 | 9 | A | 67.4 | 1 | 78 | 2.18 | 86.6 | | | 2.18 | 264.75 | 334.74 | 229.4 | 0.04278551 | 0.5023037 |
| 73.53543 | 33.30116 | 10 | K | 30.9 | 3 | 164 | 15.7 | 0.0793 | | | 15.7 | 83.621 | 114.1 | 3.6244 | 0.1967697 | 0.7239103 |
| 73.53403 | 33.30114 | 11 | KQ | 2829 | 1 | 11137 | 7.37 | 96.2 | 15.4 | 4.02 | 15.4 | 221.13 | 296.49 | 5.2402 | 0.1610984 | 12.31593 |
| 73.53486 | 33.29745 | 12 | K | 43 | 2.24 | 302 | 14.8 | 49.3 | | | 14.8 | 208.74 | 128.49 | 81.112 | 0.10109965 | 0.7948932 |
| 73.54082 | 33.29121 | 13 | H | 79.5 | 3.18 | 74.6 | 28.9 | 29447 | | | 28.9 | 33.301 | 18.269 | 424.41 | 0.42739946 | 0.5001808 |
| 73.54763 | 33.29791 | 14 | QH | 1623 | 6.52 | 27.4 | 13.8 | 3.69 | 29 | 1565 | 29 | 86.53 | 2.4952 | 3.1223 | 0.50766689 | 1.1437113 |
| 73.54723 | 33.30394 | 15 | A | 0.0061 | 9.07 | 0.0118 | 3.89 | 8.42 | | | 3.89 | 128.51 | 1.5232 | 7.7814 | 1816.54626 | 0.5474083 |
| 73.5459 | 33.30543 | 16 | K | 79.2 | 1 | 161 | 1.87 | 38.1 | | | 1.87 | 69.96 | 41.575 | 44.744 | 0.02424117 | 0.5595667 |
| 73.55583 | 33.29978 | 17 | H | 8.85 | 1 | 1.47 | 1.67 | 1452 | | | 1.67 | 2.7218 | 123.04 | 290.26 | 1.24904877 | 0.9903612 |
| 73.55072 | 33.30709 | 18 | HK | 2.15 | 1 | 0.704 | 7.72 | 5.79 | 15.4 | 0.928 | 15.4 | 16.219 | 21.905 | 15.36 | 11.4310254 | 0.074516 |
| 73.55811 | 33.29636 | 19 | K | 0.14 | 7.5 | 31.7 | 129 | 19.2 | | | 129 | 78.445 | 1.8726 | 1.2277 | 57.6408292 | 6.3269644 |
| 73.54027 | 33.30305 | 20 | K | 55.8 | 3.18 | 465 | 29 | 31.4 | | | 29 | 140.67 | 206.65 | 203.48 | 0.11935484 | 0.7873473 |
| 73.53842 | 33.29643 | 21 | Q | 53.1 | 1.56 | 16.6 | 45.9 | 0.641 | | | 45.9 | 31.633 | 825.44 | 1.3689 | 2.79443877 | 0.5240234 |

## 4. Discussion

### 4.1 Data Interpretation

The resistivity data have been interpreted quantitatively as well as qualitatively.

### 4.2 Qualitative Interpretation

#### 4.2.1 Apparent resistivity

The variations of apparent resistivity with depth is an important factor for indication of groundwater. The iso-resistivity mapping is helpful in delineating areas with variable groundwater quality [24], [25]. The apparent resistivity values at 30, 60 and 90 m depth ranges from 1.2277 to 825.44 Ωm. A comparison of these maps is shown in the Fig. 3.

**Table 2:** Modified longitudinal conductance/ protective capacity rating [30]

| Longitudinal Conductance (mhos) | Protective Capacity Rating |
|---|---|
| > 10 | Excellent |
| 5 – 10 | Very Good |
| 0.7 – 4.9 | Good |
| 0.2 – 0.69 | Moderate |
| 0.1 – 0.19 | Weak |
| < 0.1 | Poor |

The northwestern and southern parts of the map are characterized by highest apparent resistivity values. The low apparent resistivity values in the central part of study area are due to the presence of fresh water in the near surface strata.

### 4.3 Quantitative Interpretation

#### 4.3.1 Longitudinal conductance

The conductance along the bedding plane direction through 1 m column is called longitudinal conductance. It is symbolized by S (in Ω) [26], [27] The Ohm's Law defines the current flow whereas by Darcy's Law groundwater flow is controlled and a both hydraulic and electric parameters relationship is widely accepted [28].

$$S=h1/\rho1=h2/\rho2$$

$$S=\sum_{1=1}^{n} h/\mathrm{PI} \qquad (1)$$

Where "ρ" designates the resistivity of the layer and "h" is the thickness of the layer. The thick succession generally indicated by higher "S" values should given a great importance in groundwater evaluation. Fig. 4 illustrates the total longitudinal conductance map of study area. The conductance values ranges between 0 to 1800 Siemen. The values of conductance increases towards the central part of the project area. Since, the resistivity naturally decreases and conductance increases indicating towards the potential groundwater aquifers [29].

The overburden protective capability of an aquifer is directly proportional to its hydraulic conductivity. Thick clayey content which obstructs fluid movement is distinguished by low hydraulic conductivities, low resistivities and low unit longitudinal conductance [30]. The ratings of protective capacity are presented in Table 2. The clay overburden unit longitudinal conductance have been evaluated using these values (Table 2).

Fig. 5 shows the unit longitudinal conductance map of the study area. The interpretation of aquifer vulnerability shows that the protective capacity ratings at VES 1, 2, 10, 11, 12, 20 and 21 are poor, which shows that these regions are categorized by thin or no shale layers. It therefore implies that the aquifer in these sites are vulnerable to contamination. Similarly, the protective capacity at VES 3 is weak, at 3 and 18 are moderate, at 2 is good and excellent at 8, 15 and 19 respectively. It implies that the vulnerability risk is low at these locations. It has been proved that at least 10 m thick layer of shale is necessary to ensure good protective capacity for groundwater [31].

#### 4.3.2 Transverse resistance

The properties resistive and conducting layers are delineated by transverse resistance and longitudinal conductance respectively [28]. This is the total resistance through a 1 m column cut perpendicular to the plane. It is denoted by T (in Ωm−1) [26], [27]:

$$T= h\rho + h\rho + \dots\dots\dots hp$$

$$T=\sum_{1=1}^{N} hi\mathrm{PI}$$

$$T=\sum_{1=1}^{N} Ti \qquad (2)$$

Where "ρ" and "h" are true resistive and thickness respectively and "N" is the number of layers in the section. T indicates the transmissivity and higher T values are directly proportional to the aquifer transmissivity (Fig. 6). The maximum values of transverse resistance indicating the low groundwater potential zone. Conductance naturally increases, indicating the potential groundwater aquifers [29], [32].

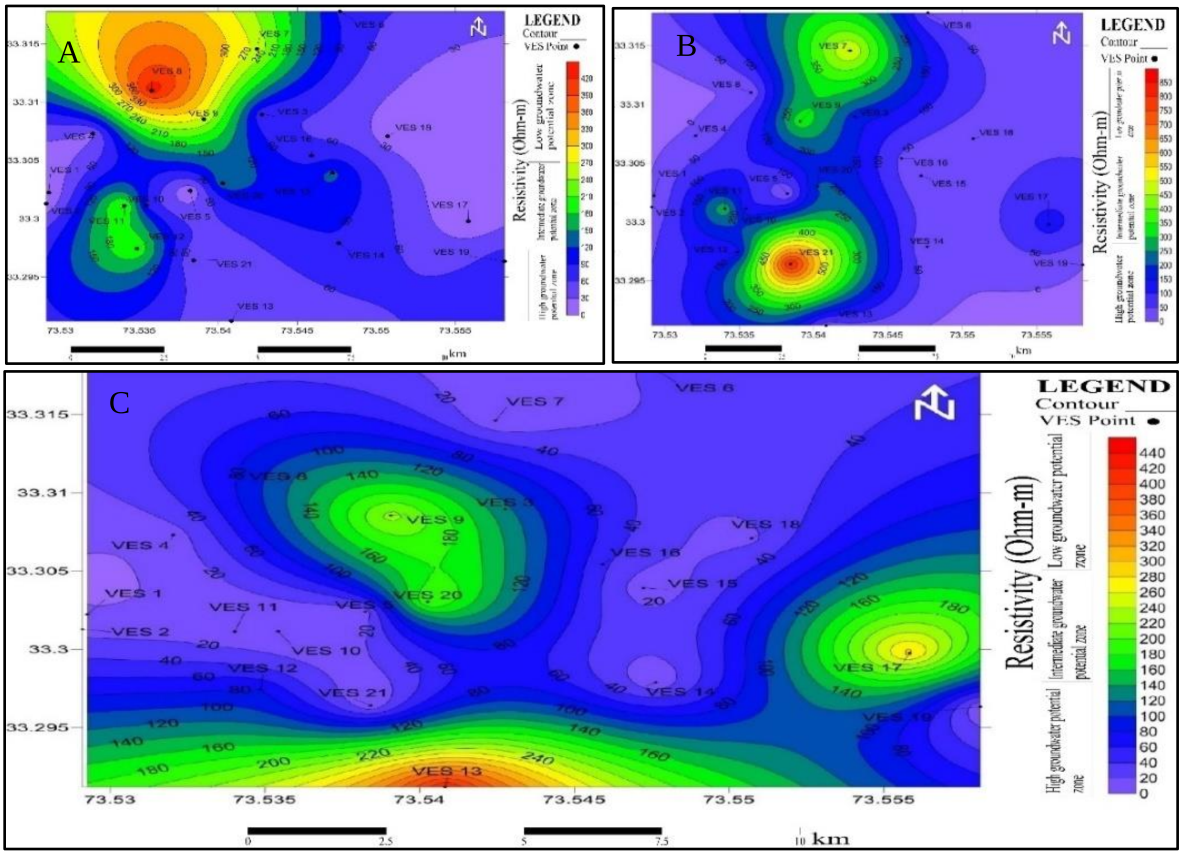


**Fig. 3:** Comparison of iso-resistivity maps at different electrode spacings. A. Apparent resistivity map at 30 m electrode spacing. B. Apparent resistivity map at 60 m electrode spacing. C. Apparent resistivity map at 90 m electrode spacing

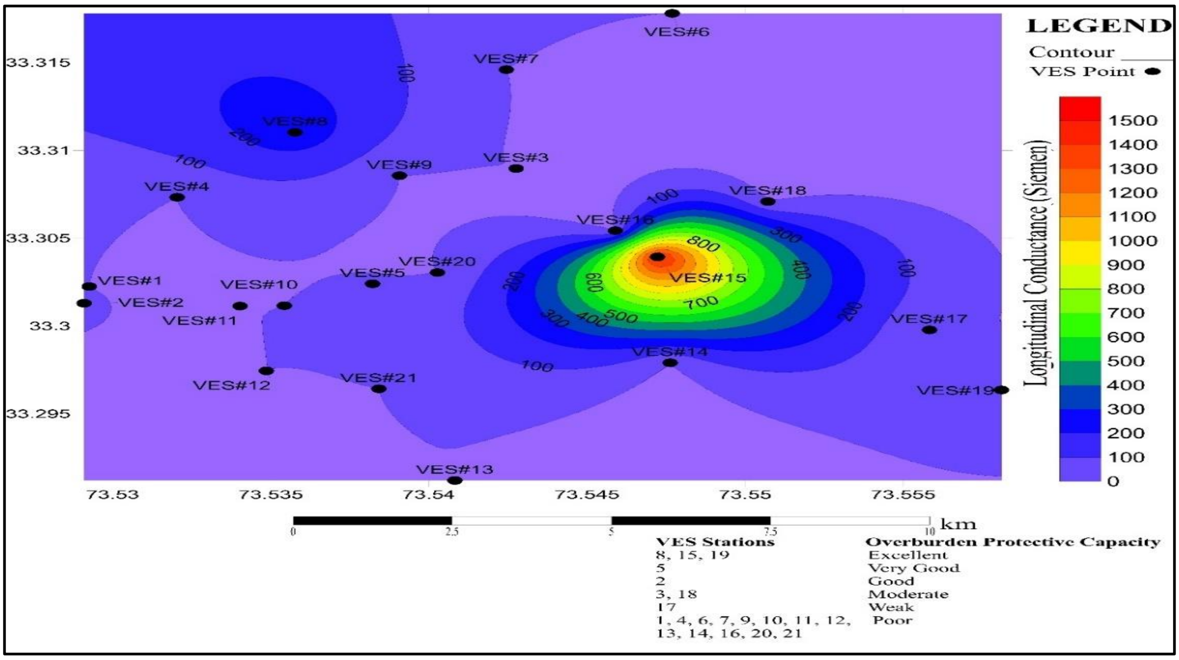


**Fig. 4:** Total longitudinal conductance map of the study area

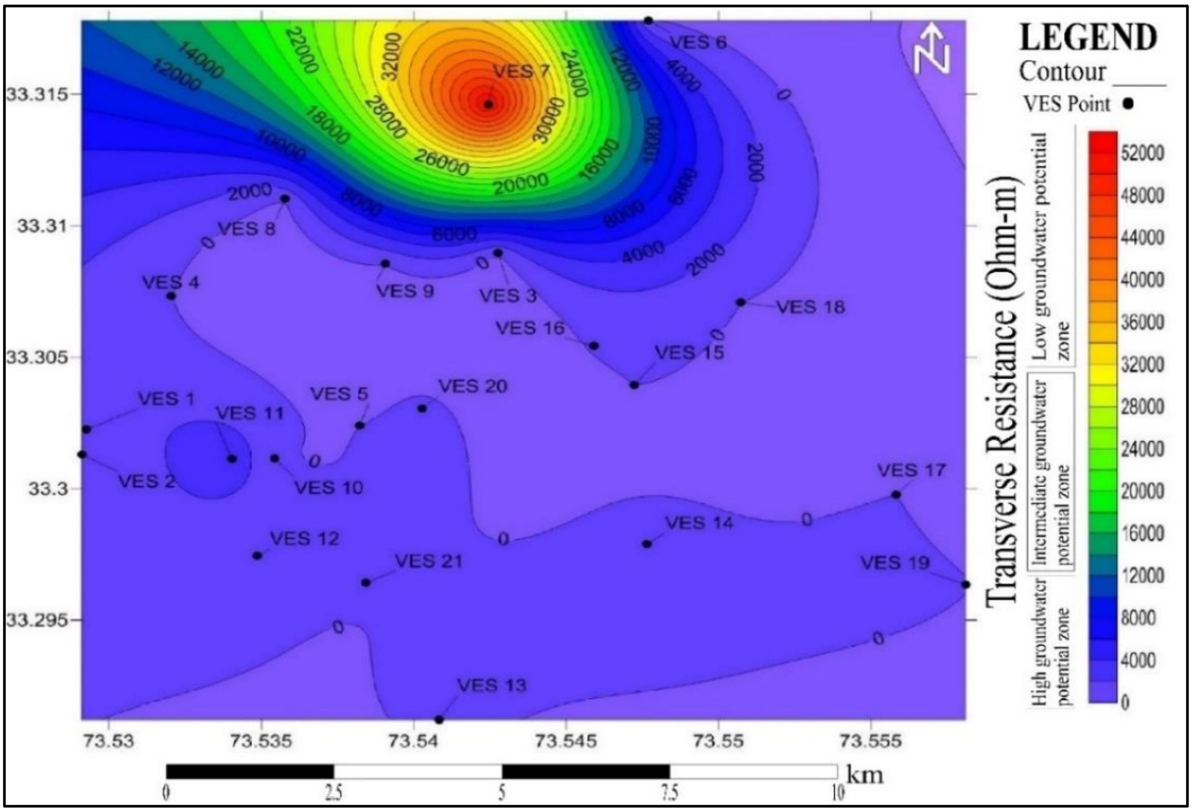


**Fig. 5:** Unit longitudinal conductance map of the study area

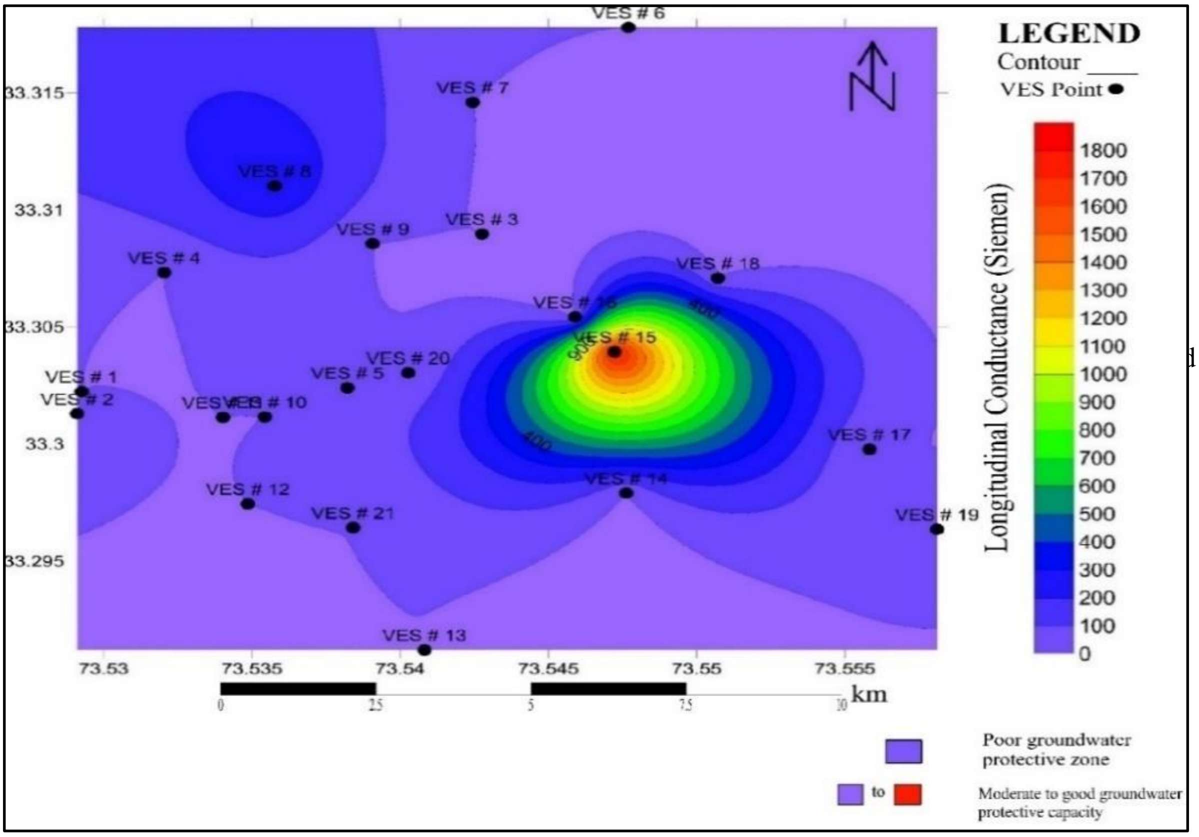


**Fig. 6:** Transverse resistance map of the study area

### 4.3.3 Land cover maps of the study area

Landsat 8 imagery of 15th Sept. 2016, Latitude 33.17677º N and Longitude 74.43642º E, Satellite Path: 149, Satellite Row: 37 with cloud cover of 3.14 % and Scene ID "LC81490372016259LGN00" was acquired from USGS Earth Explorer.

This image has 30 m resolution and was used for land cover extraction. Different types of corrections i.e., Geometric and Radiometric Corrections were performed on Landsat 8 imagery in ENVI (5.3). This imagery was further enhanced by using Calibration and DOS (Dark Object Subtraction) tools. The land cover map was prepared at the end with 5 classes (Fig. 7). This map clearly indicates the surface distribution of water bodies in the study area (Fig. 8).

The interpreted lithological model of the study area is shown in Fig. 9. Similarly, the lithology fence diagram also reflects the 3D image of subsurface geology as shown in the Fig.10 [9].

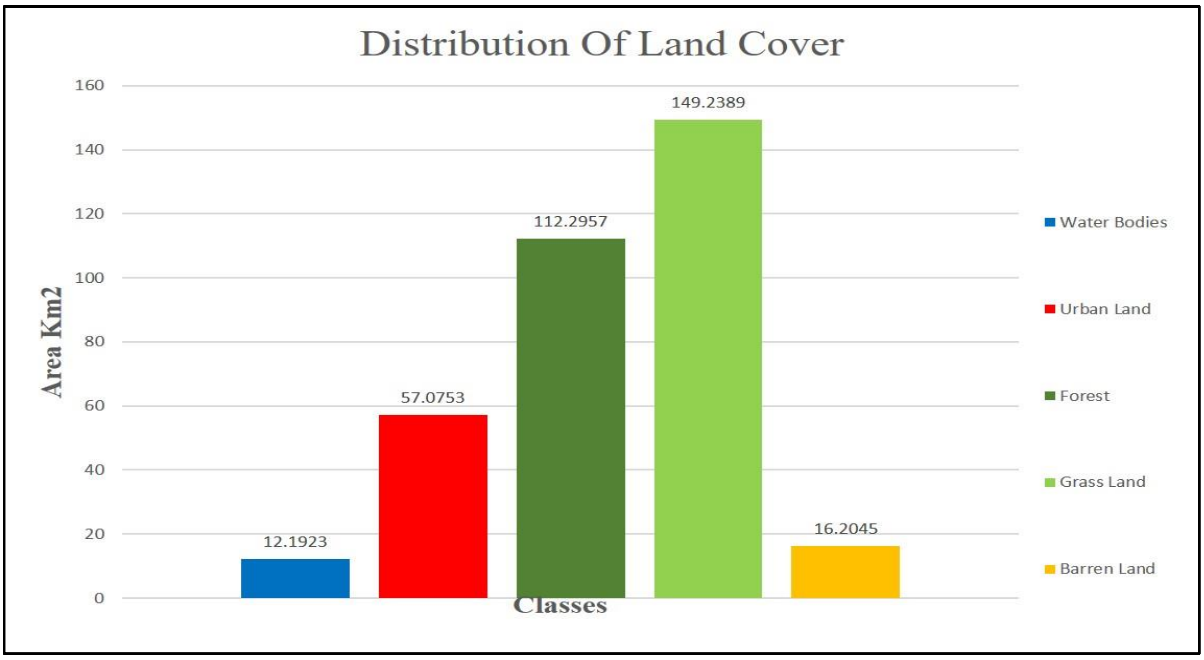


**Fig. 7:** Chart showing the distribution of land cover map

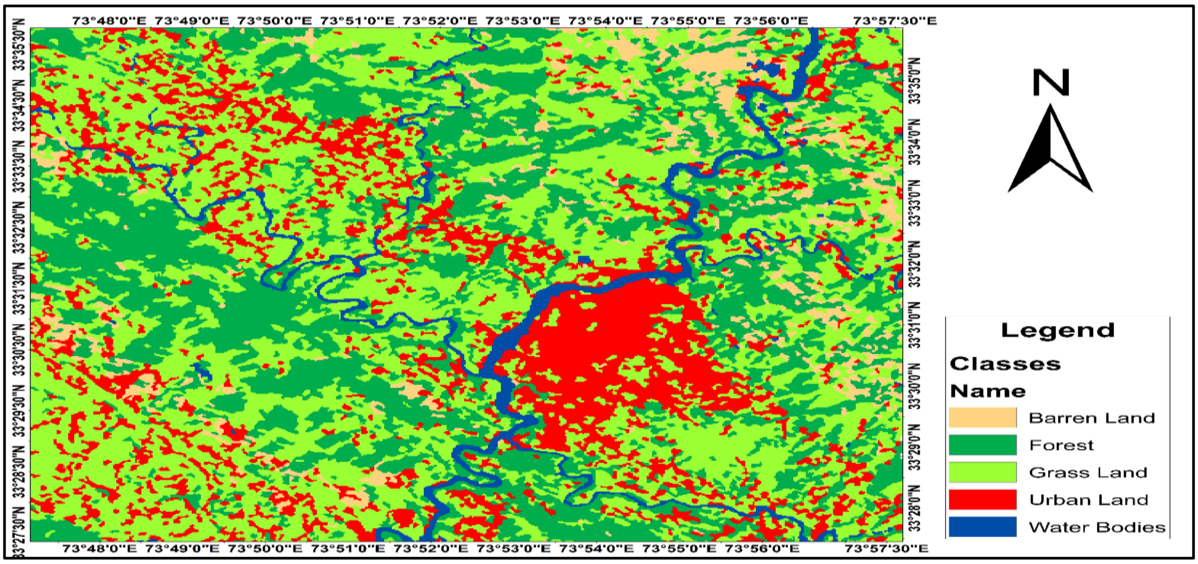


**Fig. 8:** Land cover map with rectangle showing the study area

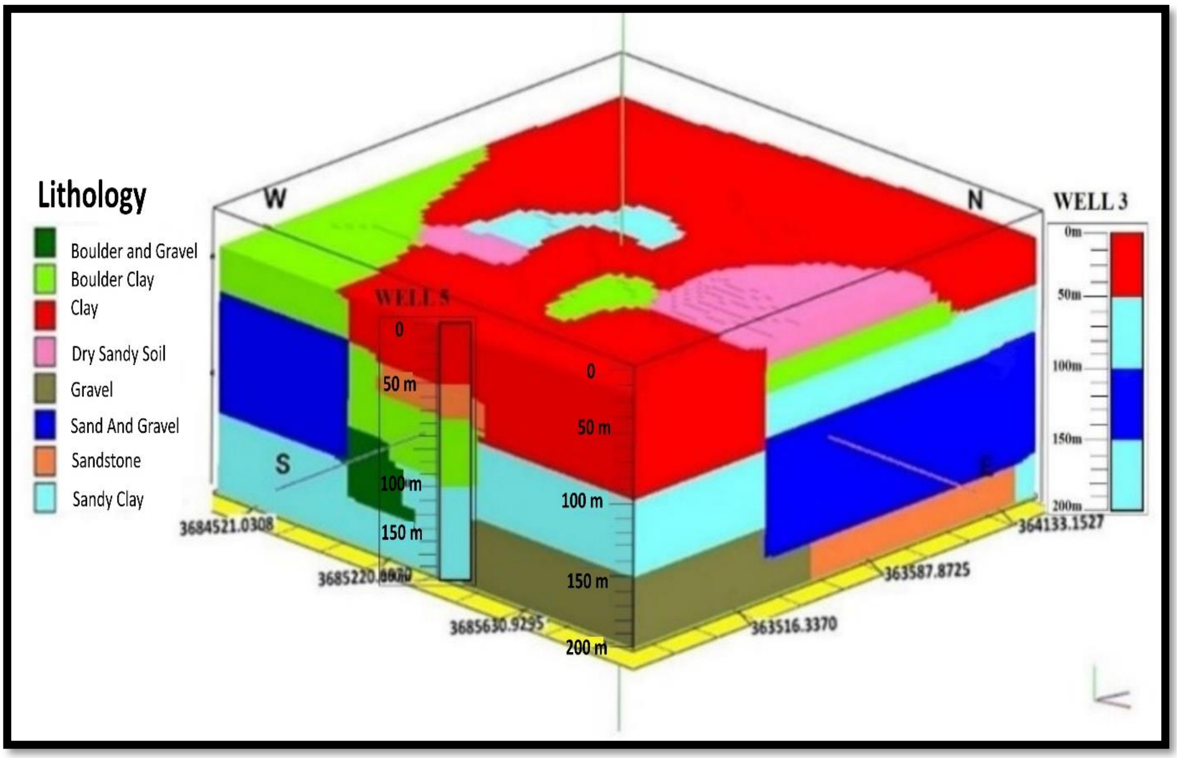


**Fig. 9:** Interpreted subsurface model of study area

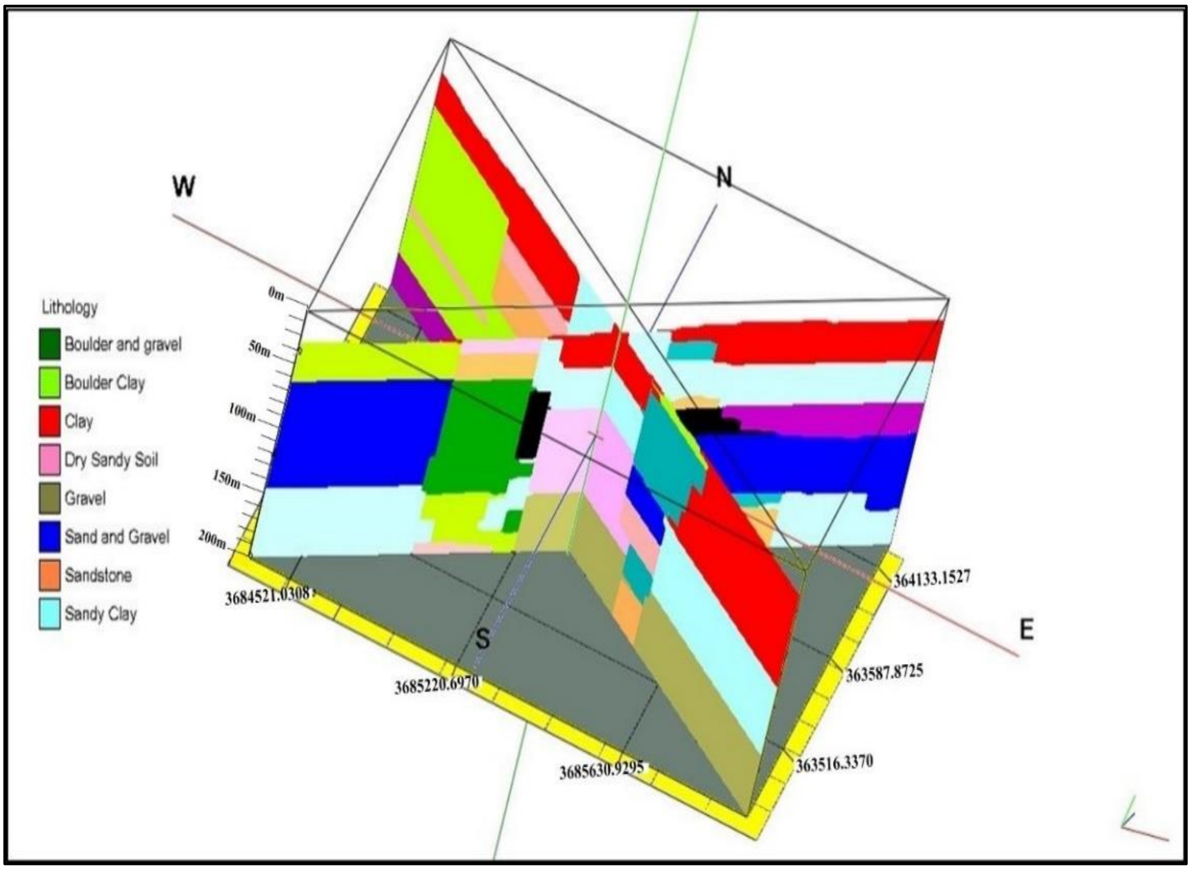


**Fig. 10:** Lithology fence diagram of study area

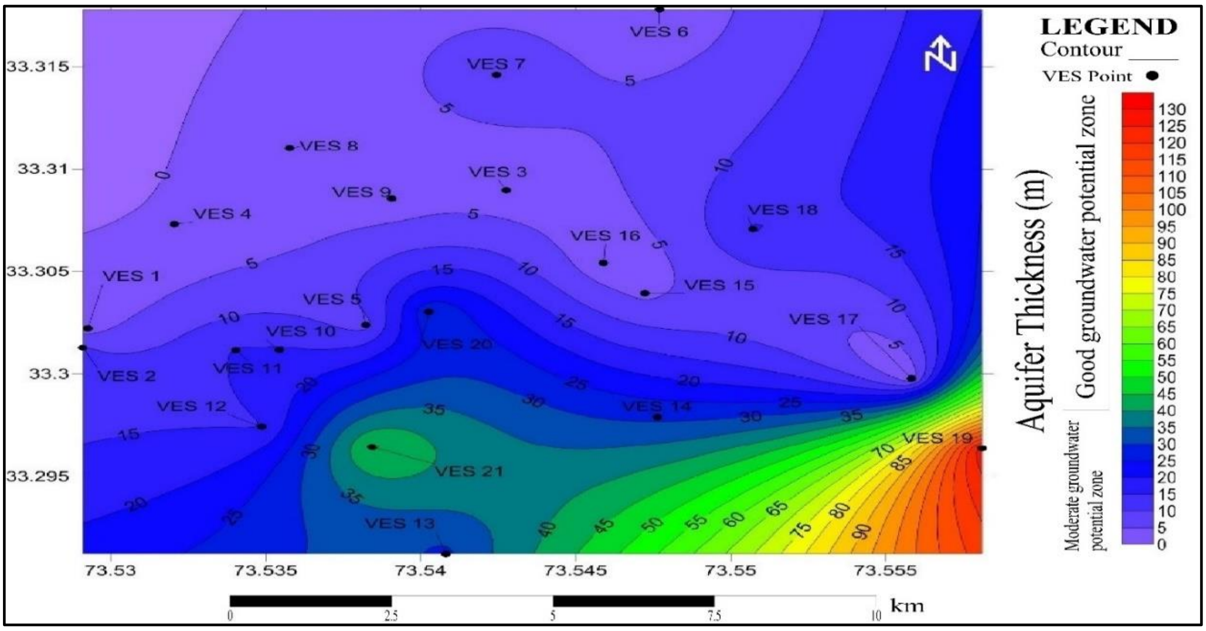


**Fig. 11:** Aquifer thickness map of the study area

The lithological model comprises the sandstone layer in the northeastern portion of the study area. The unconfined aquifers with top layers of sandstone, sand and gravels are identified in the south-western part of study area. The water bearing strata is sand and gravel, boulder clay and sandy clay.

### 4.3.4 Lithology Models of the study area

The interpreted model based on the resistivity data revealed that the study area underlies three to four layers in the subsurface. These layers are boulder clay, boulder and gravel, clay, dry sandy soil, gravel and sandstone. Aquifers are confined and unconfined in the study area but majority of aquifers are confined. Compact sandstone is also demarcated in the various parts of study area with low groundwater potential. The surface geological and hydrological information acquired by GIS lies closely to the bore hole data and computed geological model by Rockworks (17) based on the resistivity data. The 21 VES points were used for development of model and two wells data have been used for validating model. The lower values of resistivity are observed in the area of surface running water bodies due to recharging.

### 4.3.5 Aquifer thickness map

The aquifer thickness map of the project area is shown in Fig.11. Aquifer thickness map have been used for delineation of groundwater potential zones as the volume of water is directly related to the function of aquifer thickness. The red color on the map with high aquifer thickness represents good groundwater potential in the study area. The water bearing zones are categorized as good to moderate groundwater potential zones. The zone of good groundwater potential occurs at south-eastern periphery of the study area. The remaining parts of the study area were delineated as a moderate ground water potential zone.

### 4.3.6 Pseudo Section with Resistivity Section

The pseudo section plot acquired by contouring the field apparent resistivity data is an advantageous intends to present the data. The pseudo section gives an extremely surmised photo of the true subsurface resistivity appropriation. Thus, the pseudo section gives a mutilated photo of the subsurface on the grounds that the state of the shapes relies upon the kind of array utilized and in addition the true subsurface resistivity. The deliberated apparent resistivity values presentation in pictorial form can be made with the help of pseudo section and also helpful in further quantitative elucidation of an underlying strata. One basic slip-up made is to attempt to utilize the pseudo segment as a final photo of the true subsurface resistivity [33],[34]. The Figs 12-15 show the resistivity cross sections of the VES 1-21 groundwater potential zone and all the VES stations are multilayered geoelectrical stations. The minimum and maximum numbers of layers are 3 to 4.

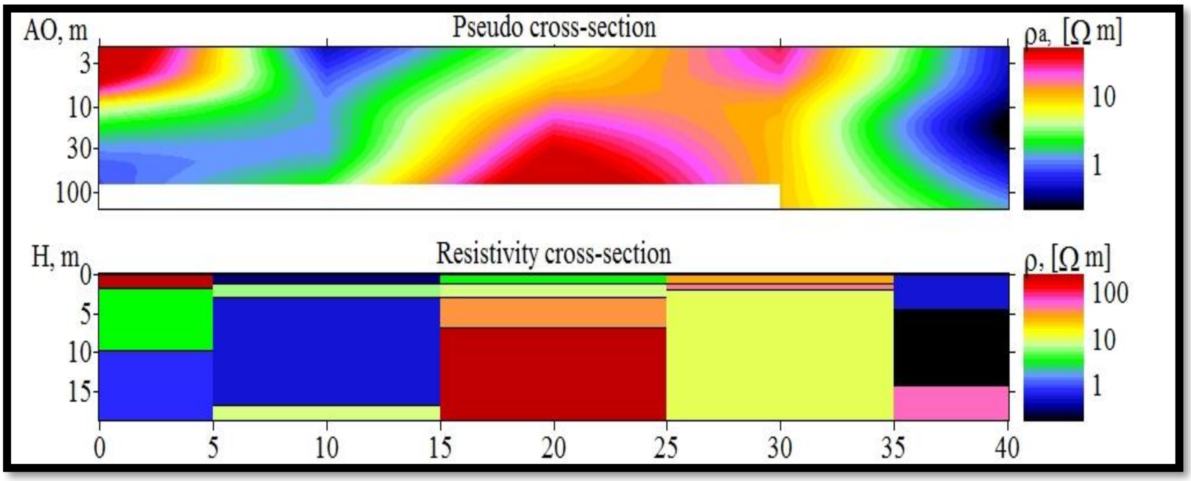


**Fig. 12:** Pseudo section and resistivity section of VES 1-5

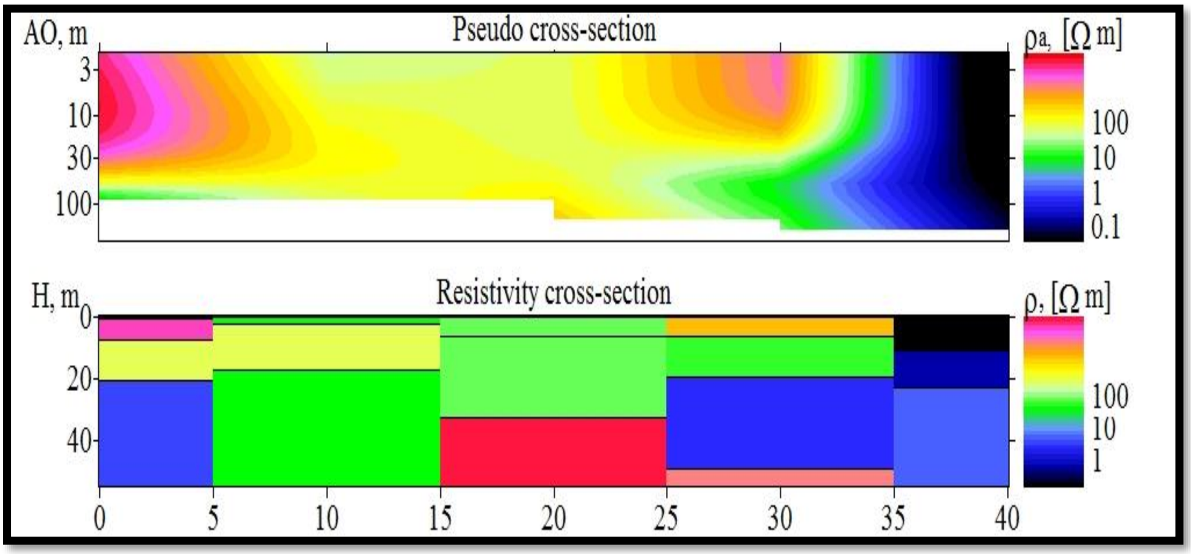


**Fig. 13:** Pseudo section and resistivity section of VES 6-10

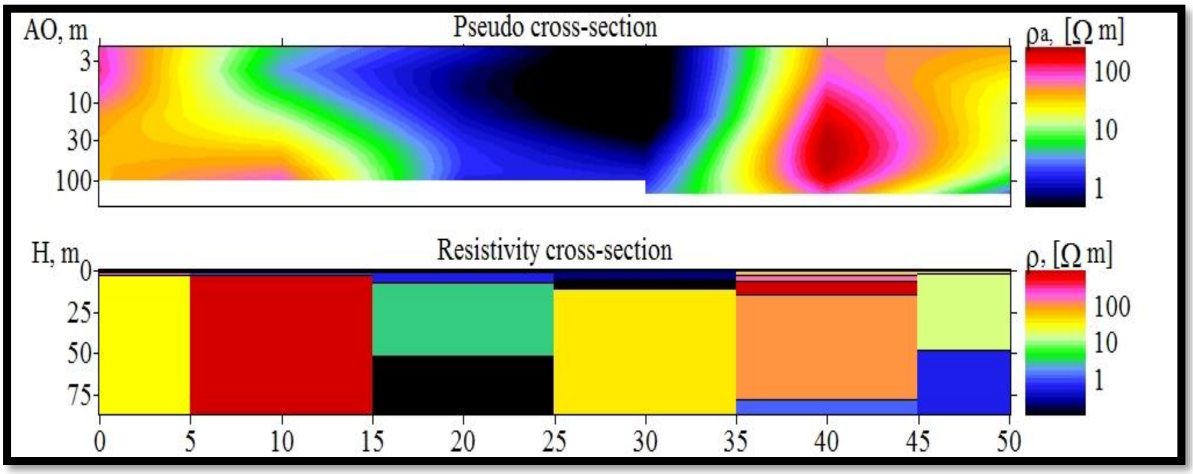


**Fig. 14:** Pseudo section and resistivity section of VES 11-15

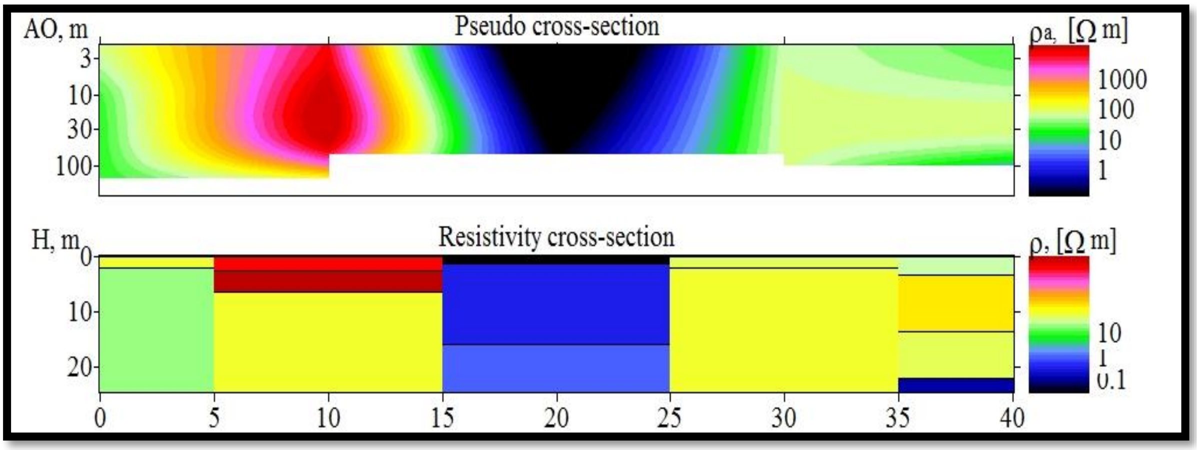


**Fig. 15:** Pseudo section and resistivity section of VES 16-21

Based on geological, hydrogeological and geoelectrical investigations, the entire profiles are underlain by the layers of boulder clay, boulder and gravel, clay, dry sandy soil, gravel and sandstone. The blue color is interpreted as the layer of clay and the yellow color is interpreted as layer of boulder clay with resistivities ranging from 16.99 Ωm-35.8 Ωm, respectively.

Similarly, the red color is interpreted as mainly the layer of weathered or fractured sandstone having resistivity ranging from 302 Ωm-29447 Ωm and orange color is interpreted as the compact sandstone/consolidated shale having resistivity values greater than 5000 Ωm respectively.

## 5. Conclusions

Vertical electrical sounding and GIS have been used for the identification of scarce groundwater resources. The conjugate techniques have been found fruitful in relating surface and subsurface water bodies. The study has revealed that the area is underlain by 3 to 4 geoelectric layers. The potential water bearing zones have been categorized into good and moderate groundwater potential zones. The aquifers in the area are mainly recharged by leakage of the surface waters and their thicknesses varies between 20 to 129 meters. It is recommended that boreholes for groundwater exploration should be drilled in the 2nd and 3rd layers. The overburden protective capacity of the aquifers are rated as poor to weak in the vicinity of VES 1, 2, 10, 11, 12, 20 and 21 south western part of the study area. The aquifers of these areas are highly vulnerable (due to high permeability of boulder clay) to the infiltration of leachate from leakage of any buried storage facility or dumps.

## 6 Acknowledgements

All the authors are grateful to the Director Institute of Geology, University of Azad Jammu and Kashmir, Muzaffarabad for financial assistance to carry out the field work in the study area.

## 7 References


[1] Niaz, A., Khan, M. R., Ijaz, U., Yasin, M. & Hameed, F. (2018). Determination of groundwater potential by using geoelectrical method and petrographic analysis in Rawalakot and adjacent areas of Azad Kashmir, sub-Himalayas, Pakistan. Arabian Journal of Geoscience, 11, 468. https://doi.org/10.1007/s12517-018-3811-0.

[2] Niaz, A., Khan, M. R., Asghar, A., Mustafa, S., Hameed, F., Umair, B. N., Khan, S., Mughal, M. S., Farooq, M. & Rizwan., M. (2017). The study of aquifers potential and contamination based on geoelectric technique and chemical analysis in Mirpur Azad Jammu and Kashmir, Pakistan. Journal of Himalayan Earth Sciences, 50 (2), 60-73.

[3] Zohdy, A., Eaton, G., Mabey, D. (1974). Application of surface geophysics to groundwater investigations. *Techniques of Water-Resources Investigation of the United States Geological Survey*. Vol. 2. pp 116-119.

[4] Gokhan, G., Blkaya, C., Erhan, Z., Yurkadul, A.(2007). Investigation of shallow alluvial aquifer using Geoelectrical methods. *Journal of Environmental Geology*. Vol. 46. pp 1283-1290.

[5] Saraf, A.K., Choudhury, P.R. (1997). Integrated Application of Remote Sensing and GIS Groundwater Exploration in Hard Rock Terrain, Proceedings of *International Symposium on Emerging Trends in Hydrology, Department of Hydrology, Roorkee, India.*

[6] Ahmad, S., Bhatti, S.S, Shahid, B.A., Khan, M.A. (2007). Framework for Selecting Spate Irrigation Systems and Interactive Focus Group Dialoguesin Baluchistan, Pakistan. (1) TA-4560.

[7] Omosuyi, G., Adeyemo, O., Adegoke, A.O. (2007). Investigation of groundwater prospect using geoelectric and electromagnetic sounding at Afunbiowo near Akurea Southwestern Nigeria. *Pacific Journal of Sciences and Technology*. Vol. 8(1). Pp 172-182.

[8] Bernstone, C., Dahlin, T., Ohlsson, T., Hogland, W. (2000). DC-resistivity mapping of internal landfill structures: two pre-excavation surveys. Environmental Geology. Vol. 39. pp 360-371.

[9] Niaz, A., Khan, M.R., Mustafa, S., Hameed, F. (2016). Determination of aquifer properties and vulnerability mapping by using geoelectrical investigation of parts of Sub-Himalayas, Bhimber, Azad Jammu and Kashmir, Pakistan. Quaternary Journal of Engineering Geology and Hydrogeology. Vol. 49. pp 36-46.

[10] El-Qady, G. (2006). Exploration of a geothermal reservoir using geoelectrical resistivity inversion case study at Hammam Mousea, Sinai, Egypt. Case study at hummam mousea Sinai. *Egyptian Journal of Geophysics and Engineering*. Vol. 3. pp 114-121.

[11] Kelly, W.E., Stanisly, M. (1993). Applied geophysics in hydrogeological and engineering practice.Elsevier, Amesterdam. pp 292.

[12] Olorunfemi, M.O., Meshida, E.A. (1987). Engineering geophysics and its application in engineering site investigation- (case study from Ilelfe area) *The Nigerian Engineer*. Vol. 22(2). pp 57-66.

[13] Oseji, J.O., Atakpo, E.A., Okolie, E.C. (2005). Geoelectric investigation of the aquifer characteristics and groundwater potential in Kwale, Delta state, Nigeria. *Journal of Applied Sciences and Environmental Management*. Vol. 9. pp 157-160.

[14] Barker, R.D. (1980). Application of geophysics in groundwater investigations, Water Surv. Vol. 84. pp 489-492.

[15] Bernard, J., Valla, P. (1991). Groundwater exploratio in fissured media with electric andVLF metods, Geoexploration., Vol. 27. pp 81- 91.

[16] Nowroozi, A., Horrocks, B., Henderson, P. (1999). Saltwater intrusion into the fresh water aquifer in the eastern shore of Virginia: a reconnaissance electrical resistivity survey. *Journal of Applied Geophysics*. Vol. 42. pp 1-22.

[17] Chukwuma, E.C., Orakwe, L.C., Anizoba, D.C., Amaefule, D.O., Odoh, C.C., Nzediwgwu, C. (2015). Geo-electric groundwater vulnerability assessment of overburden aquifers at Awka in Anambra State, South-eastern Nigeria. *European Journal of Biotechnology and Bioscience*. Vol. 3(1). pp 29-34.

[18] Niaz, A., Khan, M. R., Asghar, A., Mustafa, S. & Hameed, F., (2013). Determination of groundwater potential in Mirpur Azad Jammu and Kashmir, Pakistan using geoelectric method vertical electrical sounding. International Journal of Scientific & Engineering Research, 4, 2229-5518.

[19] Van-Overmeeren, R. (1989). Aquifer boundaries explored by geoelectrical measurements in the coastal plain of Yemen. *A Case of Equivalence. Geophysics*. Vol. 54. pp 38-48.

[20] Nisar, B. U., Khan, M. R., Khan, S., Farooq, M., Rizwan, M., Ahmed, K. A., Razzaq, S. S. &Niaz, A., (2018). Quaternary Paleo-depositional Environments in relation to Ground water occurrence in lesser Himalayan Region, Pakistan. Journal of Himalayan Earth Sciences, 51(1), 99-112.

[21] Shah, S.M.I. (2009). Stratigraphy of Pakistan. Memoirs of the Geological Survey of Pakistan. Vol. 22. pp 293-298.

[22] Zananiri, I., Memou, T., Lachanas, G. (2006). Vertical electrical sounding survey at the central part of the Kos Island, Aegean, Greece. Geoscience**.** pp 411-413.

[23] Sultan, S.A., Mekhemer, H.M., Santos, F.A.M., Abd-Alla, M. (2009). Geophysical

measurement for subsurface mapping and groundwater exploration at the central part of Sinai Peninsula, Egypt. *Arabian Journal for Science and Engineering.* Vol. 34. pp 103-119.

[24] Pal, S.K., Majumdar, R.K. (2001). Determination for groundwater potential zones using Iso-resistivity map in the alluvial areas of Munger District, Bihar. Journal of Earth Science., Vol. 1(4). pp 16-26.

[25] Arulprakasam, R., Siva, K., Gowtham, B. 2014). Electrical Resistivity Technique for demarcation of groundwater quality zones in Parts of Vanur block, Villupuram District, Tamil. *International Journal of Geology and Agriculture Environmental Sciences*. Vol. 2(1). pp 28-30.

[26] Parasnis, D.S. (1979). Principles of Applied Geophysics, John Wiley and Sons, New York, N.Y., pp 275.

[27] Nwanko, C., Nwasu, L., Emujakporue, G. (2011). Determination of Dar Zarrouk parameters for assessment of groundwater potential: case study of Imo State, southeastern Nigeria. *Journal of Economics and Sustainable Development*. Vol. 2(8). pp 57-71.

[28] Slater, L. (2007). Near surface electrical characterization of hydraulic conductivity from petrophysical properties to aquifer geometries. *Surveys in Geophysics*. Vol. 28. pp 167-169.

[29] Gowd, S.S. (2004). Electrical resistivity survey to delineate the groundwater potential aquifers in Peddavanka watershed, Anantapur District, Andhra Pradesh. *Indian Journal of Environmental Geology*. Vol. 46. pp 118-131.

[30] Henriet, J.P. (1976). Direct application of the Dar Zarrouk parameters in groundwater surveys. *Geophysical Prospects*. Vol. 24(2). pp 344-353.

[31] Walker, L.S., Gexin, C., Yongsuk, H. (2009). Colloidal and Bacterial Deposition: Role of Gravity Department of Chemical andEnvironmental Engineering, University of California, Riverside, California Langmuir. Vol. 26(1). pp 314-319.

[32] Joseph, O.C. (2012). Vertical electrical sounding (VES) methods to delineate potential groundwater aquifers in Akobo area, Ibadan, South-western, Nigeria. *Journal of Geology and Mineralogical Resources*. Vol. 4(2). pp 35-42.

[33] Loke, M.H. (2004). Electrical imaging surveys for environmental and engineering studies.

[34] Yungul, S.H. (1996). Electrical methods in geophysical exploration of sedimentary basin. Chapman and Hill, U.K: 152.